BRAIN
ORIGINAL ARTICLE

Enhancing cognitive performance prediction by white matter hyperintensity connectivity assessment

Marvin Petersen,[1] Mirthe Coenen,[2] Charles DeCarli,[3] Alberto De Luca,[2,4] Ewoud van der Lelij,[2] Alzheimer's Disease Neuroimaging Initiative, Frederik Barkhof,[5,6] Thomas Benke,[7] Christopher P. L. H. Chen,[8,9,10] Peter Dal-Bianco,[11] Anna Dewenter,[12] Marco Duering,[12,13] Christian Enzinger,[14,15] Michael Ewers,[12] Lieza G. Exalto,[2] Evan M. Fletcher,[3] Nicolai Franzmeier,[12] Saima Hilal,[9,16] Edith Hofer,[17,18] Huiberdina L. Koek,[2,19] Andrea B. Maier,[8,9,10] Pauline M. Maillard,[3] Cheryl R. McCreary,[20] Janne M. Papma,[21,22,23] Yolande A. L. Pijnenburg,[24] Reinhold Schmidt,[17,18] Eric E. Smith,[20] Rebecca M. E. Steketee,[24] Esther van den Berg,[21,22] Wiesje M. van der Flier,[24] Vikram Venkatraghavan,[24] Narayanaswamy Venketasubramanian,[10,25] Meike W. Vernooij,[21,26,27] Frank J. Wolters,[26,27] Xin Xu,[10,28] Andreas Horn,[29,30] Kaustubh R. Patil,[31,32] Simon B. Eickhoff,[31,32] Götz Thomalla,[1] J. Matthijs Biesbroek,[2,33] Geert Jan Biessels[2] and Bastian Cheng[1]

See O'Sullivan (https://doi.org/10.1093/brain/awae377) for a scientific commentary on this article.

White matter hyperintensities of presumed vascular origin (WMH) are associated with cognitive impairment and are a key imaging marker in evaluating brain health. However, WMH volume alone does not fully account for the extent of cognitive deficits and the mechanisms linking WMH to these deficits remain unclear. Lesion network mapping (LNM) enables us to infer if brain networks are connected to lesions and could be a promising technique for enhancing our understanding of the role of WMH in cognitive disorders. Our study employed LNM to test the following hypotheses: (i) LNM-informed markers surpass WMH volumes in predicting cognitive performance; and (ii) WMH contributing to cognitive impairment map to specific brain networks.

We analysed cross-sectional data of 3485 patients from 10 memory clinic cohorts within the Meta VCI Map Consortium, using harmonized test results in four cognitive domains and WMH segmentations. WMH segmentations were registered to a standard space and mapped onto existing normative structural and functional brain connectome data. We employed LNM to quantify WMH connectivity to 480 atlas-based grey and white matter regions of interest (ROI), resulting in ROI-level structural and functional LNM scores. We compared the capacity of total and regional WMH volumes and LNM scores in predicting cognitive function using ridge regression models in a nested cross-validation. LNM scores predicted performance in three cognitive domains (attention/executive function, information processing speed, and verbal memory) significantly better than WMH volumes. LNM scores did not improve prediction for language functions. ROI-level analysis revealed that higher LNM scores, representing greater connectivity to WMH, in grey and white matter regions of the dorsal and ventral attention networks were associated with lower cognitive performance.

Measures of WMH-related brain network connectivity significantly improve the prediction of current cognitive performance in memory clinic patients compared to WMH volume as a traditional imaging marker of cerebrovascular

Received April 15, 2024. Revised August 14, 2024. Accepted September 21, 2024. Advance access publication October 14, 2024

disease. This highlights the crucial role of network integrity, particularly in attention-related brain regions, improving our understanding of vascular contributions to cognitive impairment. Moving forward, refining WMH information with connectivity data could contribute to patient-tailored therapeutic interventions and facilitate the identification of subgroups at risk of cognitive disorders.

1 Department of Neurology, University Medical Center Hamburg-Eppendorf, Hamburg 20251 Germany
2 Department of Neurology and Neurosurgery, University Medical Center Utrecht Brain Center, Utrecht 3584 CX, The Netherlands
3 Department of Neurology, University of California, Davis, CA 95616 USA
4 Division Imaging and Oncology, Image Sciences Institute, UMC Utrecht, Utrecht 3584 CX, The Netherlands
5 Department of Radiology and Nuclear Medicine, Amsterdam UMC, Vrije Universiteit Amsterdam, Amsterdam 1081 BT, The Netherlands
6 Queen Square Institute of Neurology and Centre for Medical Image Computing, University College, London WC1N 3BG, UK
7 Clinic of Neurology, Medical University Innsbruck, Innsbruck 6020, Austria
8 Department of Pharmacology, Yong Loo Lin School of Medicine, National University of Singapore, Singapore 119228, Singapore
9 Department of Psychological Medicine, Yong Loo Lin School of Medicine, National University of Singapore, Singapore 119228, Singapore
10 Memory, Aging and Cognition Center, National University Health System, Singapore 119228, Singapore
11 Department of Neurology, Medical University Vienna, Vienna 1090, Austria
12 Institute for Stroke and Dementia Research (ISD), LMU University Hospital, LMU Munich, Munich 81377, Germany
13 Medical Image Analysis Center (MIAC) and Department of Biomedical Engineering, University of Basel, Basel 4051, Switzerland
14 Division of General Neurology, Department of Neurology, Medical University Graz, Graz 8036, Austria
15 Division of Neuroradiology, Interventional and Vascular Radiology, Department of Radiology, Medical University of Graz, Graz 8036, Austria
16 Saw Swee Hock School of Public Health, National University of Singapore and National University Health System, Singapore 119228, Singapore
17 Division of Neurogeriatrics, Department of Neurology, Medical University of Graz, Graz 8036, Austria
18 Institute for Medical Informatics, Statistics and Documentation, Medical University of Graz, Graz 8036, Austria
19 Department of Geriatric Medicine, University Medical Center Utrecht, Utrecht University, Utrecht 3584 CX, The Netherlands
20 Department of Clinical Neurosciences and Radiology and Hotchkiss Brain Institute, University of Calgary, Calgary AB T2N 4N1, Canada
21 Alzheimer Center Erasmus MC, Erasmus MC University Medical Center, Rotterdam 3015 GD, The Netherlands
22 Department of Neurology, Erasmus MC University Medical Center, Rotterdam 3015 GD, The Netherlands
23 Department of Internal Medicine, Erasmus MC University Medical Center, Rotterdam 3015 GD, The Netherlands
24 Alzheimer Center Amsterdam, Department of Neurology, Amsterdam Neuroscience, Amsterdam UMC, Vrije Universiteit Amsterdam, Amsterdam 1081 BT, The Netherlands
25 Raffles Neuroscience Center, Raffles Hospital, Singapore 119228, Singapore
26 Department of Radiology and Nuclear Medicine, Erasmus MC University Medical Center, Rotterdam 3015 GD, The Netherlands
27 Department of Epidemiology, Erasmus MC University Medical Center, Rotterdam 3015 GD, The Netherlands
28 School of Public Health and the Second Affiliated Hospital of School of Medicine, Zhejiang University, Zhejiang 310009, China
29 Department of Neurology with Experimental Neurology, Charité - Universitätsmedizin Berlin, Movement Disorders and Neuromodulation Unit, Berlin 10117, Germany
30 Department of Neurology, Psychiatry, and Radiology, Center for Brain Circuit Therapeutics, Brigham and Women's Hospital, Harvard Medical School, Boston, MA 02115, USA
31 Institute for Systems Neuroscience, Medical Faculty, Heinrich-Heine University Düsseldorf, Düsseldorf 40225, Germany
32 Institute of Neuroscience and Medicine, Brain and Behaviour (INM-7), Research Center Julich, Jülich 52428, Germany
33 Department of Neurology, Diakonessenhuis Hospital, Utrecht 3582 KE, The Netherlands

Correspondence to: Marvin Petersen, MD
Department of Neurology, University Medical Center Hamburg-Eppendorf, Martinistraße 52
Hamburg 20246, Germany
E-mail: mar.petersen@uke.de

Correspondence may also be addressed to: Bastian Cheng, MD
E-mail: b.cheng@uke.de

Keywords: vascular cognitive impairment; white matter hyperintensities; dementia; lesion network mapping; magnetic resonance imaging; cerebral small vessel disease

Introduction

Cerebral small vessel disease (CSVD) is a major driver of vascular cognitive impairment (VCI) and often also contributes to dementia with a primary neurodegenerative or mixed pathology.[1] White matter hyperintensities (WMH) are the signature imaging marker of CSVD, and mark sites of white matter disintegration caused by microangiopathic axonal loss and demyelination.[2,3] However, a comprehensive understanding of mechanisms linking WMH to their broad range of clinical manifestations, specifically cognitive impairment, is still lacking.

Although there is a well documented association between WMH volumes and cognitive functions at the group level, the association between WMH volume and symptom severity demonstrates considerable variability with some individuals exhibiting fewer symptoms despite high WMH burden and vice versa.[4] The apparent complexity of this relationship underscores the need for improved techniques for disease quantification to more accurately predict individual cognitive impairment for effective diagnostics and ultimately targeted treatment of VCI patients.[5] An important part of the variation in the impact of WMH on cognition may be explained by loco-regional WMH effects. For example, lesion-symptom inference techniques have linked cognitive impairment to WMH located in strategic white matter regions, independent of total WMH volume.[4,6-8]

However, these findings might not fully reflect the complexity of CSVD-related cognitive impairment, which is thought to emerge from disturbances in the interplay of large-scale brain networks involving cortical and subcortical grey matter areas, interconnected by white matter tracts.[9,10] In recent years, advanced imaging analysis models have been developed to comprehensively capture lesion effects on brain circuitry.[11] Specifically, lesion network mapping (LNM) techniques capitalize on advanced neuroimaging to map lesions on reconstructions of the human brain network.[12] By that, a lesion's connectivity to different brain regions can be quantified—i.e. the lesion's network embedding is measured—allowing one to infer which regions are disconnected.[11,13] LNM measures have been associated with clinical symptoms in a variety of neurological disorders that can be understood as 'disconnection syndromes', such as stroke or multiple sclerosis.[13-15]

Here, we propose LNM as a technique to quantify WMH connectivity for improved prediction of cognitive performance in VCI. We employ LNM on a large scale, multicentre dataset, integrating cognitive test results and MRI-based WMH segmentations from 3485 patients of 10 memory clinic cohorts through the Meta VCI Map Consortium.[6,16] Our hypotheses are twofold: (i) LNM-based measures of WMH connectivity surpass WMH volumes in predicting cognitive performance; and (ii) WMH contributing to cognitive deficits map to specific brain networks that functionally determine their symptom profile.

Materials and methods

Study population

Methodological details are illustrated in Fig. 1. We examined previously harmonized, cross-sectional clinical and imaging data of 3485 patients from 10 memory clinic cohorts of the Meta VCI Map Consortium.[6,16] Meta VCI map is a multi-site collaboration for conducting meta-analyses of strategic lesion topography in vascular cognitive impairment. The memory clinic cohorts included in this study comprise the Alzheimer Center Erasmus MC (ACE, $n = 52$, The Netherlands), Alzheimer's Disease Neuroimaging Initiative (ADNI, $n = 994$, USA),[17] UC Davis Alzheimer's Disease Center Diversity Cohort (AUCD, $n = 641$, USA),[18] BrainIMPACT ($n = 53$, Canada),[19] Functional Assessment of Vascular Reactivity (FAVR, $n = 47$, Canada),[19] Harmonization ($n = 207$, Singapore),[4] Prospective Dementia Registry (PRODEM, $n = 367$, Austria),[20] TRACE-VCI ($n = 821$, The Netherlands),[21] Utrecht Memory Clinic Cohort (UMCC, $n = 227$, The Netherlands) and VASCAMY ($n = 76$, Germany). All cohorts include patients assessed at outpatient memory clinics for cognitive symptoms, undergoing structural MRI alongside neuropsychological tests of cognitive performance. Patients with cognitive impairment due to non-vascular, non-neurodegenerative causes (e.g. excessive alcohol use disorder, cerebral malignancies, multiple sclerosis) or monogenic disorders (e.g. CADASIL) were excluded. Further details on each cohort, including sample-specific inclusion and exclusion criteria were reported previously.[6]

Ethics approval

All cohorts received the requisite ethical and institutional approval in accordance with local regulations, which included informed consent, to allow data acquisition and sharing.[6]

Cognitive assessments

Detailed harmonization procedures, including specific test-to-domain assignments, were reported previously.[22] Neuropsychological tests from participating cohorts were norm-referenced against local norms or a healthy control group, and adjusted on the individual subject level for age, sex and education. These tests were categorized into four cognitive domains: attention/executive function, information processing speed, language and verbal memory. Within these domains, norm-referenced neuropsychological test scores were z-scored and averaged to

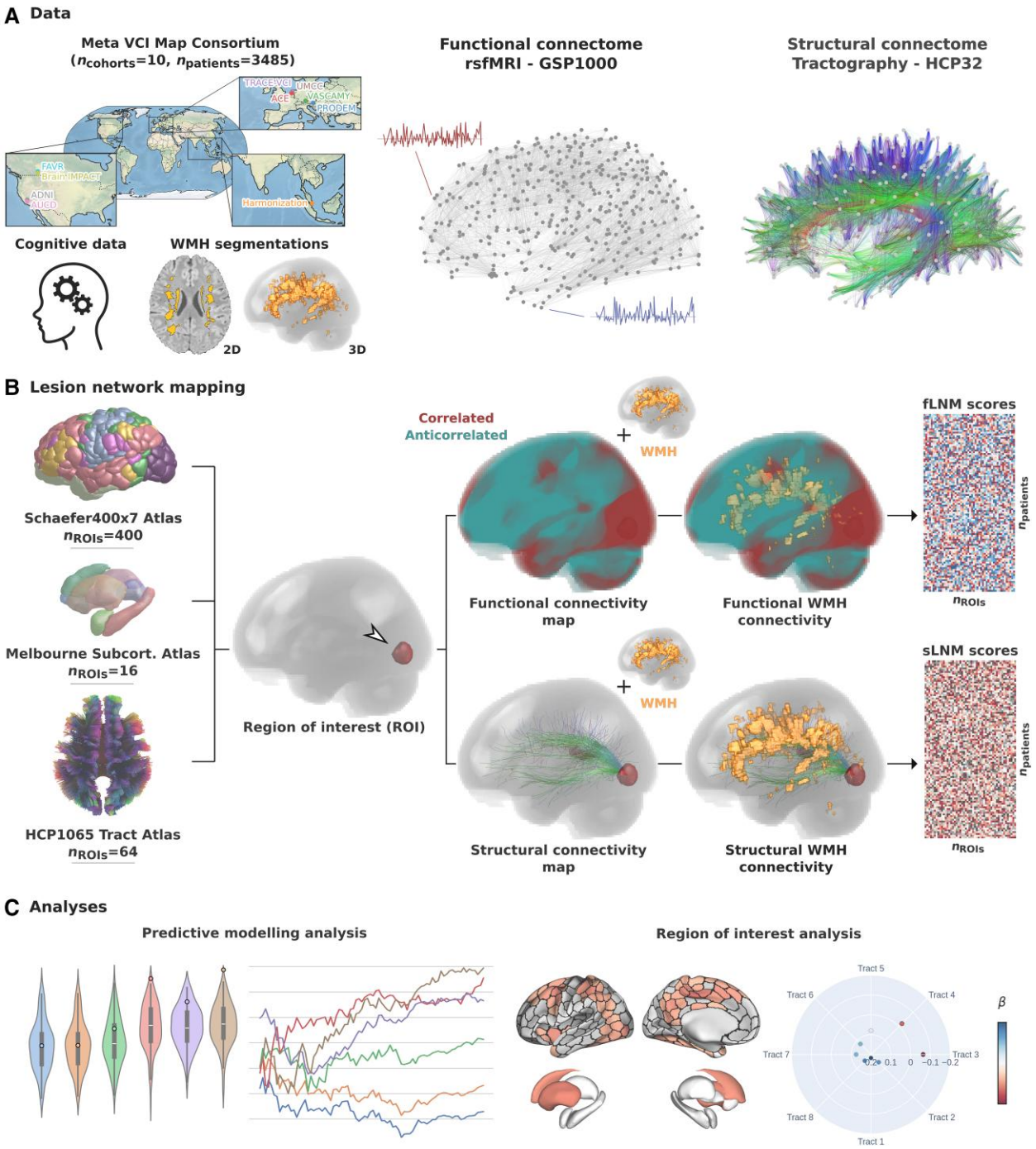

Figure 1 Methodology. (**A**) Data from 10 memory clinic cohorts of the Meta VCI Map Consortium were used including harmonized cognitive scores and WMH segmentations in MNI space. For functional lesion network mapping (fLNM) we employed the GSP1000 normative functional connectome comprising resting state fMRI (rsfMRI) data from 1000 healthy GSP participants. For structural lesion network mapping (sLNM), we used the HCP32 normative structural connectome based on diffusion-weighted imaging data from 32 healthy HCP participants, detailing the fibre bundle architecture. (**B**) LNM was performed to quantify the functional and structural connectivity of white matter hyperintensities of presumed vascular origin (WMH) to multiple regions of interest (ROIs) (Schaefer400 × 7 cortical, Melbourne Subcortical Atlas subcortical, HCP1065 white matter areas). For this, voxel-level functional and structural connectivity maps were computed for each ROI, reflecting resting state blood oxygen level-dependent (BOLD) correlations or anatomical connection strength via tractography streamlines, respectively. ROIwise LNM scores were derived by averaging voxel-level connectivity indices within the normalized WMH masks, considering only positive correlation coefficients for functional mapping. This resulted in a matrix for both fLNM and sLNM scores per ROI per patient ($n_{ROIs} \times n_{patients}$). The matrices shown in the figure are populated with random data only serving as a visual aid. (**C**) The fLNM and sLNM scores across patients were used in predictive models to estimate cognitive domain scores (predictive modelling analysis) and analysed in permutation-based general linear models to identify regions significantly influencing the cognitive domain-WMH disconnectivity relationship at the ROI level (ROI-level inferential statistics). GSP = Genomic Superstruct Project; HCP = Human Connectome Project.

obtain cognitive domain scores (z-scores), which capture individual-level cognitive domain performance relative to healthy controls.

White matter hyperintensity segmentation

WMH segmentations were provided by the participating centres or performed at the UMC Utrecht (ACE cohort). Segmentation masks were obtained applying established automated neuroimaging software on fluid-attenuated inversion recovery (FLAIR) MRI.[23] WMH segmentations were spatially normalized to the Montreal Neurological Institute (MNI)-152 template.[24] To ensure registration quality, the normalized WMH masks were visually inspected and patients with failed registrations were excluded. Furthermore, random subsamples of normalized WMH segmentations were returned to the respective participating institutions to confirm the data quality. WMH segmentation masks were used to compute the total WMH volume as well as tract-level WMH volumes for each of the 64 white matter fibre tracts of the HCP1065 Tract Atlas.[25] Details on cohort-specific segmentation and registration procedures were reported previously.[6,26]

Lesion network mapping

LNM was performed to quantify the functional and structural connectivity of WMH to cortical, subcortical and white matter regions of interest (ROIs) following previous procedures.[13,15,27,28] ROIs were defined in MNI space using the following established atlases for comprehensive brain coverage: Schaefer400 × 7 Atlas (n_{ROIs} = 400), the Melbourne Subcortical Atlas (n_{ROIs} = 16) and the HCP1065 Tract Atlas (n_{ROIs} = 64) (Fig. 1B).[25,29,30] For visualization of the investigated HCP1065 tracts, see Supplementary Fig. 1.

Functional lesion network mapping (fLNM) was conducted using a normative functional connectome, derived from resting state functional MRI (fMRI) scans of 1000 healthy individuals from the Genomic Superstruct Project (GSP1000).[31,32] Preprocessing was performed using a modified version of the Computational Brain Imaging Group (CBIG) fMRI preprocessing pipeline (https://github.com/bchcohenlab/CBIG/tree/master/stable_projects/preprocessing/CBIG_fMRI_Preproc2016), as described elsewhere.[31,33] For each ROI, we averaged blood oxygen level-dependent (BOLD) signal fluctuations across voxels within the ROI and correlated this aggregate time series with BOLD signals of all brain voxels. This process generated 1000 Pearson correlation coefficients per voxel, i.e. one for each GSP1000 subject, which were then Fischer z-transformed and averaged across subjects to create a functional connectivity map per ROI. Functional connectivity map computations were performed using the ROI masks as seeds in the 'connectome mapper' function of Lead-DBS (lead-dbs.org).[34] Subsequently, ROI-level fLNM scores were calculated by averaging positive Pearson correlation coefficients within the WMH mask, reflecting each ROI's functional connectivity to WMH.

Structural lesion network mapping (sLNM) was performed using a normative structural connectome of 32 subjects of the Human Connectome Project (HCP32).[27] The structural connectome was reconstructed by applying DSI Studio on multi-shell diffusion MRI data acquired on a MRI scanner specifically designed for high-fidelity connectome reconstruction. Streamlines resulting from whole brain tractography were normalized to MNI and aggregated across subjects.[35] Using Lead-DBS, voxel-wise structural connectivity maps were computed per atlas ROI, quantifying per voxel the number of streamlines connecting the voxel to the ROI.[34] ROI-level sLNM scores, reflecting structural connectivity between WMH and individual ROI, were determined by averaging the voxel values (representing streamline counts to the ROI) within the WMH mask.

Summarized, LNM yielded both a fLNM and sLNM score for each ROI per subject, indicating the functional and structural connectivity between WMH and ROI, respectively. In accordance with previous studies, we interpret these measures of WMH connectivity as indirect measures of disconnectivity.[11,13]

Predictive modelling analysis

To evaluate the predictive capacity of fLNM and sLNM scores, we performed a predictive modelling analysis leveraging scikit-learn (v. 1.0.2, scikit-learn.org) and julearn (v. 0.3.0, juaml.github.io/julearn).[36,37] This work defines 'prediction' in accordance with previous studies as the estimation of target variables using a trained statistical model on new unseen data—emphasizing the crucial aspect of model generalizability.[11,38,39] We note that this definition varies from those indicating longitudinal study designs used in epidemiological contexts.[40] In the analysis, six different feature sets were compared: (i) demographics (age, sex and education); (ii) total WMH volume + demographics; (iii) tract-level WMH volumes + demographics; (iv) ROI-level fLNM scores + demographics; (v) ROI-level sLNM scores + demographics; and (vi) ROI-level fLNM and sLNM scores + demographics.

For each cognitive domain, multivariable ridge regression models were trained using the abovementioned feature sets to predict cognitive domain scores. Ridge regression models include a L2 regularization, which is a technique to control the model complexity. It reduces coefficients to mitigate overfitting and to address multicollinearity improving the model's ability to generalize to unseen data. We optimized the L2 regularization through a 10-fold nested cross-validation, tuning α-values ranging from 0.001 to 1000 (α = 0.001, 0.01, 0.1, 1, 10, 100, 1000). In this procedure, the α-values were optimized within an inner cross-validation loop, while the performance of the optimized models was evaluated in an outer loop based on test data not seen during training. This method prevents bias in the assessment of predictive performance. The model performance was scored by the Pearson correlation between actual and predicted cognitive domain scores, supplemented with explained variance (R^2, coefficient of determination) and negative mean squared error as additional measures of performance. In line with best practices, explained variance was calculated via sum-of-squares formulation (using scikit-learn's *r2_score*) instead of squaring Pearson correlations.[38] Before model fitting, continuous input features were z-scored in a cross-validation consistent manner to avoid data leakage.[41] To maintain a consistent distribution of the target variable across training and test sets, we employed julearn's 'ContinuousStratifiedKFold' function for creating the folds. Cross-validations were repeated 10 times with varied random splits to minimize bias from any single split.[42] This approach yielded 100 scores for each feature-target set combination, which were compared between feature sets using a machine learning-adjusted *t*-test.[43] We repeated the predictive modelling analysis for different sample sizes (20%–100%, 1% steps, randomly sampled) to examine the robustness and sample size dependency of predictive performances. As a whole, this analysis follows current best practices of predictive modelling in neuroimaging to address overfitting as well as prevent leakage and circularity, ensuring accurate estimates of predictive validity.[38]

Region of interest-level inferential statistics

To investigate whether WMH connectivity of specific brain circuits link to impaired cognitive performance, we conducted

permutation-based testing for linear associations between regional LNM scores and cognitive domain scores in a general linear model. All statistical analyses were conducted in FSL's Permutation Analysis of Linear Models (PALM) based on MATLAB (v. 2021b) and Python 3.9.1 leveraging neuromaps (v. 0.0.5).[44-46] Statistical tests were two-sided ($n_{permutation} = 5000$), with a $P < 0.05$ as the significance threshold. To account for multiple comparisons, P-values were adjusted for family-wise error rate. General linear models were adjusted for age, sex and education. To obtain standardized β-coefficients, input variables were z-scored beforehand. As a result, β-coefficients and P-values were obtained for each cortical, subcortical and white matter ROI ($n_{ROIs} = 480$) indicating the strength and significance of the LNM score's linear association with cognitive domain scores for each ROI. To aid in interpreting the spatial effect patterns, we averaged the β-coefficients representing cortical effects in the seven intrinsic resting state networks (Yeo networks), which reflect the cerebral cortex's intrinsic functional organization.[33] The Schaefer400 × 7 Atlas assigns ROIs to these networks: visual, somatomotor, dorsal attention, ventral attention (salience), limbic, frontoparietal control and default mode network.[29] Significance was tested via spin permutations ($n_{spins} = 1000$), which represent a null model preserving the inherent spatial autocorrelation of cortical information.[47]

Sensitivity analyses

To examine if our results are driven by specific analysis design decisions, we performed multiple sensitivity analyses.

During computations of fLNM scores, we decided to only consider positive Pearson correlations of resting state BOLD signal within WMH masks following previous approaches, as the role of negative correlations is controversial.[48] However, some studies suggest biological meaning in anticorrelations of BOLD signal fluctuations.[49,50] Hence, we conducted a sensitivity analysis based on fLNM scores computed by averaging only the negative Pearson correlations in the WMH masks. We reconducted the predictive modelling analysis and ROI-level inferential statistics using these negative fLNM scores.

Moreover, previous work employs thresholding to discard potentially noisy connectivity information. To further examine the effect of thresholding on our results, we repeated the predictive modelling analysis comparing the main analysis results to fLNM and sLNM scores computed based on 25% and 50% highest voxel intensities in the WMH mask. For negative fLNM scores, the lowest 25% and 50% voxel intensities in the WMH mask were considered.

Furthermore, we tested the robustness of predictive performance across different Schaefer Atlas resolutions. Therefore, we computed LNM scores for the Schaefer100 × 7 and Schaefer200 × 7 Atlas and repeated the predictive modelling analysis based on these measures.

Last, we tested *post hoc* whether the results regarding language performance prediction could be confounded by disconnection originating from the right hemisphere. Hence, we examined if language prediction remained stable considering only left-hemispheric WMH for the LNM score computations and left-hemispheric ROIs in the predictive modelling analysis.

Supplementary analyses

Further analyses including LNM informed by the WMH penumbra,[51,52] investigation of structure-function coupling of LNM scores, voxel-level lesion network maps and voxel-based lesion-symptom mapping[53,54] are described in the Supplementary material, 'Supplementary text S2' section.

Table 1 Sample characteristics

Demographics	
Age in years, mean ± SD (*n*)	71.71 ± 8.87 (3485)
Female, *n* (%)	1737 (49.8)
Years of education, mean ± SD (*n*)	12.89 ± 4.45 (3485)
Patient ethnicity	
Afro-Caribbean, *n* (%)	198 (5.7)
Asian, *n* (%)	237 (6.8)
Caucasian/European/White, *n* (%)	1620 (46.5)
Hispanic, *n* (%)	146 (4.2)
Other, *n* (%)	52 (1.5)
Diagnosis	
Subjective cognitive impairment, *n* (%)	777 (22.30)
Mild cognitive impairment, *n* (%)	1389 (39.86)
Dementia, *n* (%)	1319 (37.85)
For dementia cases: probable aetiology	
Alzheimer's dementia, *n* (%)	764 (57.9)
Vascular dementia, *n* (%)	85 (6.4)
Frontotemporal dementia, *n* (%)	44 (3.3)
Dementia with Lewy bodies, *n* (%)	24 (1.8)
Cardiovascular risk factors	
Current smoking, *n* (%)	499 (14.3)
Previous smoking, *n* (%)	459 (13.2)
Hypertension, *n* (%)	1714 (49.2)
Hypercholesterolemia, *n* (%)	1098 (31.5)
Diabetes mellitus, *n* (%)	492 (14.1)
BMI, mean ± SD (*n*)	25.28 ± 4.75 (640)
Comorbidities	
Atrial fibrillation, *n* (%)	98 (2.8)
History of prior stroke, *n* (%)	244 (7.0)
History of prior transient ischaemic attack (TIA), *n* (%)	62 (1.8)
History of prior other vascular events, *n* (%)	715 (20.5)
Imaging	
WMH volume in ml, median [IQR] (*n*)	6.19 [14.21] (3485)
Cognitive function	
Mini-Mental State Examination, mean ± SD (*n*)	25.0 ± 4.7 (3327)
Attention/executive function, *z*, mean ± SD (*n*)	−1.12 ± 1.10 (3446)
Information processing speed, *z*, mean ± SD (*n*)	−0.96 ± 1.61 (2417)
Language, *z*, mean ± SD (*n*)	−1.08 ± 1.86 (2041)
Verbal memory, *z*, mean ± SD (*n*)	−1.48 ± 1.30 (3242)

BMI = body mass index; IQR = interquartile range; SD = standard deviation; WMH = white matter hyperintensities of presumed vascular origin; *z* = harmonized *z*-score.

Results

Sample characteristics

The pooled study sample of 3485 patients had a mean age of 71.7 ± 8.9 years and 49.8% were female. Among patients, 777 (22.3%) had subjective cognitive impairment, 1389 (39.9%) had mild cognitive impairment, and 1319 (37.9%) had dementia. Further details on the sample characteristics can be found in Table 1. A heat map of WMH distribution can be found in Supplementary Fig. 3.

Predictive modelling analysis

To evaluate if information on WMH network connectivity exceeds the predictive capacity of volumetric WMH metrics for cognitive performance, we first computed regional fLNM and sLNM scores, that capture the functional and structural connectivity profile of

WMH. We then employed ridge regression for predictive modelling. Model performance was assessed via Pearson correlation (r) of predicted and actual cognitive domain scores averaged across folds. All models incorporated age, sex and education (demographics) as features to establish a performance baseline. The corresponding results are visualized in Fig. 2A. In summary, compared to WMH volumes, LNM scores significantly improved cognitive function prediction in all domains, except language. In detail, the predictive performance achieved by the demographics-only model was $r = 0.312$ for attention/executive function, $r = 0.239$ for information processing speed, $r = 0.404$ for language and $r = 0.305$ for verbal memory. Models informed by total or tract-wise WMH volumes achieved a predictive performance of $r = 0.341$–0.365 for attention/executive function, $r = 0.247$–0.250 for information processing speed, $r = 0.404$–0.416 for language and $r = 0.327$–0.356 for verbal memory. For the prediction of attention/executive function, models informed by LNM scores exhibited a significantly higher predictive performance than models informed by volumetric WMH measures (LNM: $r = 0.399$–0.410 versus WMH volume: $r = 0.341$–0.365; adjusted t-test, all $P < 0.05$). LNM-informed models also better predicted information processing speed (LNM: $r = 0.310$–0.316 versus WMH volume: $r = 0.247$–0.250, adjusted t-test, all $P < 0.05$) as well as verbal memory (LNM: $r = 0.390$–0.408 versus WMH volume: $r = 0.327$–0.356; adjusted t-test, all $P < 0.05$). Across these domains, the best prediction was achieved by models incorporating both structural and functional LNM scores. For attention/executive function, comparing the improvement from the demographics-based model to the model informed by total WMH volume ($0.341 - 0.312 = 0.029$) with the improvement to the model based on both LNM modalities ($0.410 - 0.312 = 0.098$), the usage of fLNM and sLNM scores amounts to a 3.38-fold increase ($0.098/0.029 = 3.38$) in added predictive performance. Considering both LNM modalities for predicting information processing speed and verbal memory amounted to 7.00-fold and 4.68-fold increase in predictive performance, respectively. For the prediction of language domain scores, performance between LNM-informed models and WMH volume measures did not differ significantly (LNM: $r = 0.380$–0.409 versus WMH volume: $r = 0.404$–0.416, all $P > 0.05$). See Supplementary material, Sections S4 and S5 for predictive modelling results using explained variance and negative mean squared error as scoring methods. Details on regional averages of LNM scores are shown in Supplementary Fig. 6.

To test the robustness of prediction results, we repeated the analysis in randomly chosen subsamples of increasing sizes (Fig. 2B). For attention/executive function and verbal memory, LNM-informed models started to consistently exceed WMH volume-based models at ~50% (attention/executive function: $n = 1723$, verbal memory: $n = 1712$; note that data availability differed between cognitive domain scores) of the sample size. For information processing speed, LNM-informed models surpassed WMH volume-based models at ~25% ($n = 604$) of the sample size. Regarding language, LNM-informed models approximated the performance of WMH volume-based models with increasing sample sizes. For all cognitive domain scores, predictive performance in the sample size range 80–100% showed high stability and only minor increases indicating saturation.

Contextualization of WMH connectivity: region of interest analysis

We tested if WMH connectivity to specific brain circuits links to cognitive performance by quantifying the association between regional LNM scores (grey matter regions and white matter tracts) and cognitive domain scores adjusting for age, sex and education.

Results of the general linear model linking LNM scores in cortical and subcortical grey matter regions to cognitive domain scores are shown in Fig. 3. Higher fLNM scores (i.e. increased WMH connectivity) in cortical regions of the dorsal attention and ventral attention networks were linked to lower attention/executive function and verbal memory (Fig. 3A and C). Regarding information processing speed, the extent of the effect was limited to several cortical brain areas mapping to the dorsal attention network (Fig. 3B). In terms of sLNM, higher scores in the dorsal attention network were significantly associated with lower attention/executive function and information processing speed (Fig. 3D and E). Again, information processing speed showed a spatially more limited effect pattern. The relationship of regional sLNM and verbal memory scores showed a different spatial distribution mapping to the ventral attention, frontoparietal and default mode network (Fig. 3F). The cortical and subcortical LNM scores showed no significant association with the language domain score.

The results for anatomically predefined white matter tracts are shown in Fig. 4. For tract-level fLNM, lower cognitive performance in attention/executive function, information processing speed and verbal memory was most strongly linked to higher fLNM scores in association and projection tracts connecting the parietal cortex (Fig. 4B): the middle longitudinal fasciculus (MdLF), parietal corticopontine tract (CPT), dorsal, medial and ventral sections of the superior longitudinal fasciculus (SLF 1–3), the parietoparahippocampal cingulate (C parietoparahipp.). For attention/executive function, a significant negative effect was also evident for the right arcuate fasciculus (AF). For verbal memory, significant negative effects were additionally found for the corticobulbar tract (CBT) and frontal aslant tract (FAT).

Regarding tract-level sLNM, lower attention/executive function and verbal memory were significantly associated with higher sLNM scores in association and projection tracts connecting frontal regions (Fig. 4C): the frontoparahippocampal cingulate (C parietoparahipp.), parolfactory cingulate (C parolfactory), the superior longitudinal fasciculus (SLF 1–3), frontoparietal cingulate (C frontoparietal), anterior thalamic radiation, anterior corticostriatal pathways (CS anterior), uncinate fascicle, frontal corticopontine tract (CPT frontal). For attention/executive function, a significant negative effect was also evident for the right AF. Furthermore, higher verbal memory scores were significantly linked to higher sLNM scores in the fornices. Information processing speed showed a significant negative association with sLNM scores in the right medial superior longitudinal fasciculus (SLF 2) and frontoparahippocampal cingulate (C frontoparahipp.). Tract-level LNM scores showed no significant association with language function. For plots displaying all tract-level associations refer to Supplementary Figs 7 and 8.

The spatial effect patterns, i.e. β-coefficient maps, showed considerable overlap with 26 of 28 effect pattern pairs being significantly correlated (see Supplementary Fig. 9 for a correlation matrix).

Sensitivity analyses

Predictive modelling results were stable when using negative fLNM scores (based on anti-correlations in resting state fMRI measures) and when including a 25% or 50% thresholding step (Supplementary Fig. 10). Exploratory ROI-level inferential statistics based on negative fLNM scores indicated that lower attention/executive function and information processing speed were more significantly associated with more negative fLNM scores in the

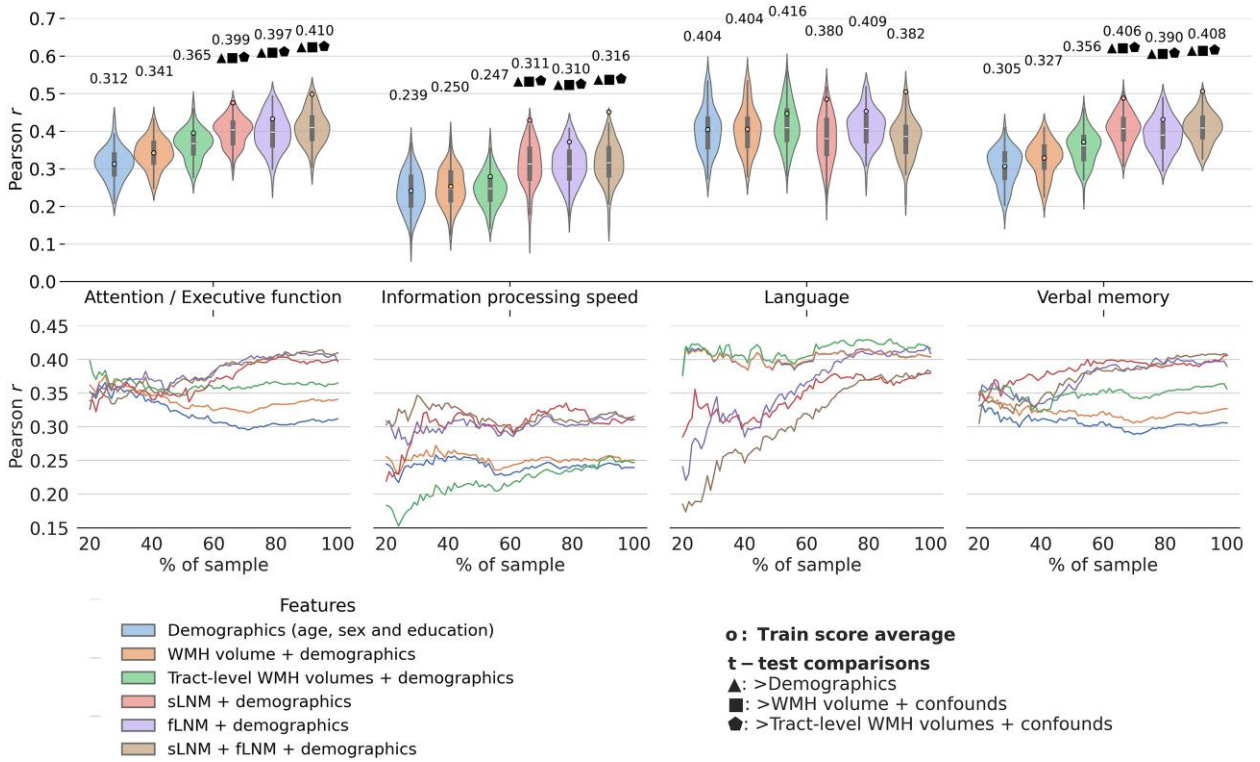

Figure 2 Predictive modelling analysis. Violin plots illustrate prediction outcomes across cognitive domains. Each violin displays the distribution of Pearson correlations (between actual and predicted cognitive domain performance; 10-fold cross-validation × 10 repeats = 100 folds → 100 Pearson correlations) for a model informed by a different feature set. The higher the Pearson correlation, the higher the prediction performance. Blue = demographics (age, sex and education); orange = total WMH volume + demographics; green = tract-level WMH volumes + demographics; red = sLNM scores + demographics; purple = fLNM scores + demographics; brown = sLNM scores + fLNM scores + demographics. Average Pearson correlations are indicated above each violin, with coloured dots showing training score averages. Geometric symbols denote *t*-test results comparing LNM-based models against demographics and WMH volume-based models: filled triangle ▲ indicates significantly higher Pearson correlation than demographics, filled square ■ indicates significantly higher Pearson correlation than WMH volume + demographics; and filled pentagon ⬟ indicates significantly higher Pearson correlation than tract-level WMH volume + demographics. Below the violin plots, performance curves display the average Pearson correlations across folds, for subsets randomly sampled in sizes ranging from 20% to 100% of the entire dataset. Line colours match the corresponding violin plots in **A**, which display predictive modelling results for the full sample size. Again, higher Pearson correlation indicates higher prediction performance. fLNM = functional lesion network mapping; sLNM = structural lesion network mapping; WMH = white matter hyperintensities of presumed vascular origin.

default mode network (Supplementary Figs 11 and 12). Predictive modelling results were also robust if considering the Schaefer100 × 7 and Schaefer200 × 7 Atlas during LNM score computations instead of the Schaefer400 × 7 Atlas (Supplementary Fig. 13). Of note, models informed by Schaefer100 × 7 and Schaefer200 × 7 fLNM scores and demographics predicted language function significantly better than models informed by demographics and WMH volume measures. Predictive modelling of language performance only informed by left-hemispheric LNM scores showed stable results (Supplementary Fig. 14). In sum, our results were robust across sensitivity analyses.

Supplementary analyses

Supplementary analyses are detailed in the Supplementary material, 'Supplementary text S2' section. WMH penumbra-based LNM scores slightly improved predictive performance compared to original LNM scores for attention/executive function ($r = 0.406$–0.416), information processing speed ($r = 0.318$–0.328) and verbal memory ($r = 0.402$–0.414) (Supplementary Fig. 15). Functional and structural LNM scores were significantly correlated across ROIs and across subjects (Supplementary Fig. 16) with a mean correlation coefficient of 0.50 ± 0.26. Voxel-level lesion network maps indicating white matter regions that contribute to variance in cognitive domain function are shown in Supplementary Figs 17 and 18. Voxel-based lesion-symptom mapping based on sparse canonical correlation analysis revealed significant voxel-level associations between WMH occurrence and cognitive performance across domains. Significant associations were located bilaterally in periventricular regions for all cognitive domains. The corresponding lesion-symptom maps can be found in Supplementary Fig. 19. Average prediction performance achieved by voxel-based lesion-symptom mapping was lower compared to LNM-informed models: average $r = 0.250$ for attention/executive function, $r = 0.196$ for information processing speed, $r = 0.204$ for language and $r = 0.310$ for verbal memory (Supplementary Fig. 20).

Discussion

In a large multicentric sample of memory clinic patients, we conducted an in-depth examination of the link between functional and structural LNM scores and cognitive performance. We report two main findings: (i) both structural and functional LNM scores, capturing WMH connectivity, significantly improved the prediction of cognitive performance compared to WMH volume in the domains attention/executive function, information processing speed and verbal memory; and (ii) WMH connectivity associated with lower cognitive performance, predominantly mapped to the dorsal and ventral attention networks.

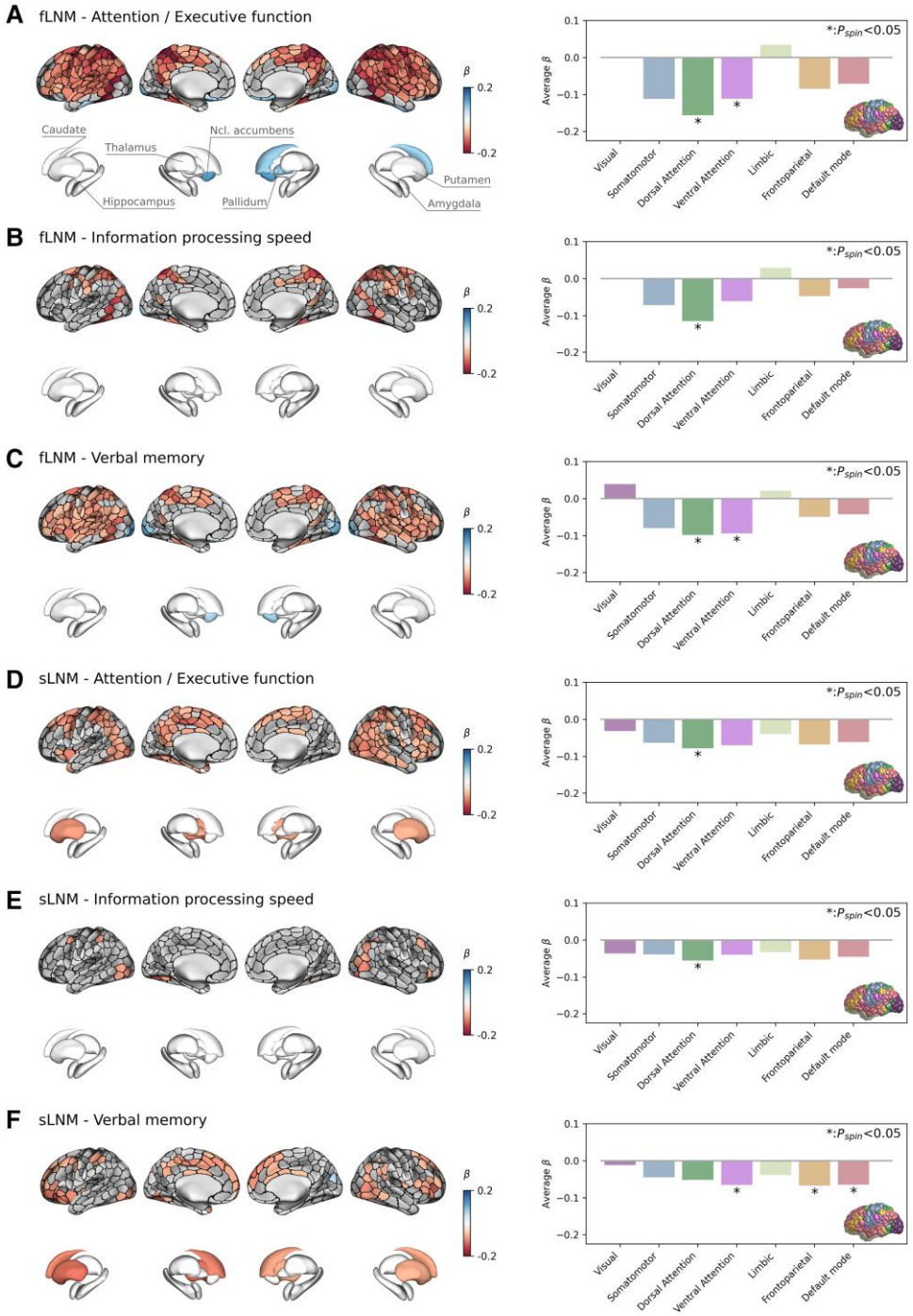

Figure 3 Inferential statistics results of cortical and subcortical grey matter. Anatomical plots on the *left* display the regional relationship between lesion network mapping (LNM) scores and cognitive domain scores. Regions of interest (ROIs) in which LNM scores across participants were significantly associated with cognitive domain scores after family-wise error rate correction are highlighted by colours encoding β-coefficients from general linear models: a negative β (red) denotes that a higher regional LNM score, i.e. higher WMH connectivity, is associated to a lower performance in individual cognitive domains; a positive β (blue) indicates that a higher regional LNM score is linked to a higher cognitive domain performance. Bar plots on the *right* display the corresponding β-coefficients averaged in the canonical (Yeo) resting state functional connectivity networks. The brain in the *bottom right* indicates the regional distribution of the canonical resting state networks with colours corresponding to the bars. Statistical significance was assessed using spin permutations. Each row corresponds with a different combination of lesion network mapping modality and cognitive domain: (**A**) fLNM—attention/executive function; (**B**) fLNM—information processing speed; (**C**) fLNM—verbal memory; (**D**) sLNM—attention/executive function; (**E**) sLNM—information processing speed; and (**F**) sLNM—verbal memory. fLNM = functional lesion network mapping; P_{spin} = *P*-value derived from spin permutations; sLNM = structural lesion network mapping; WMH = white matter hyperintensities of presumed vascular origin.

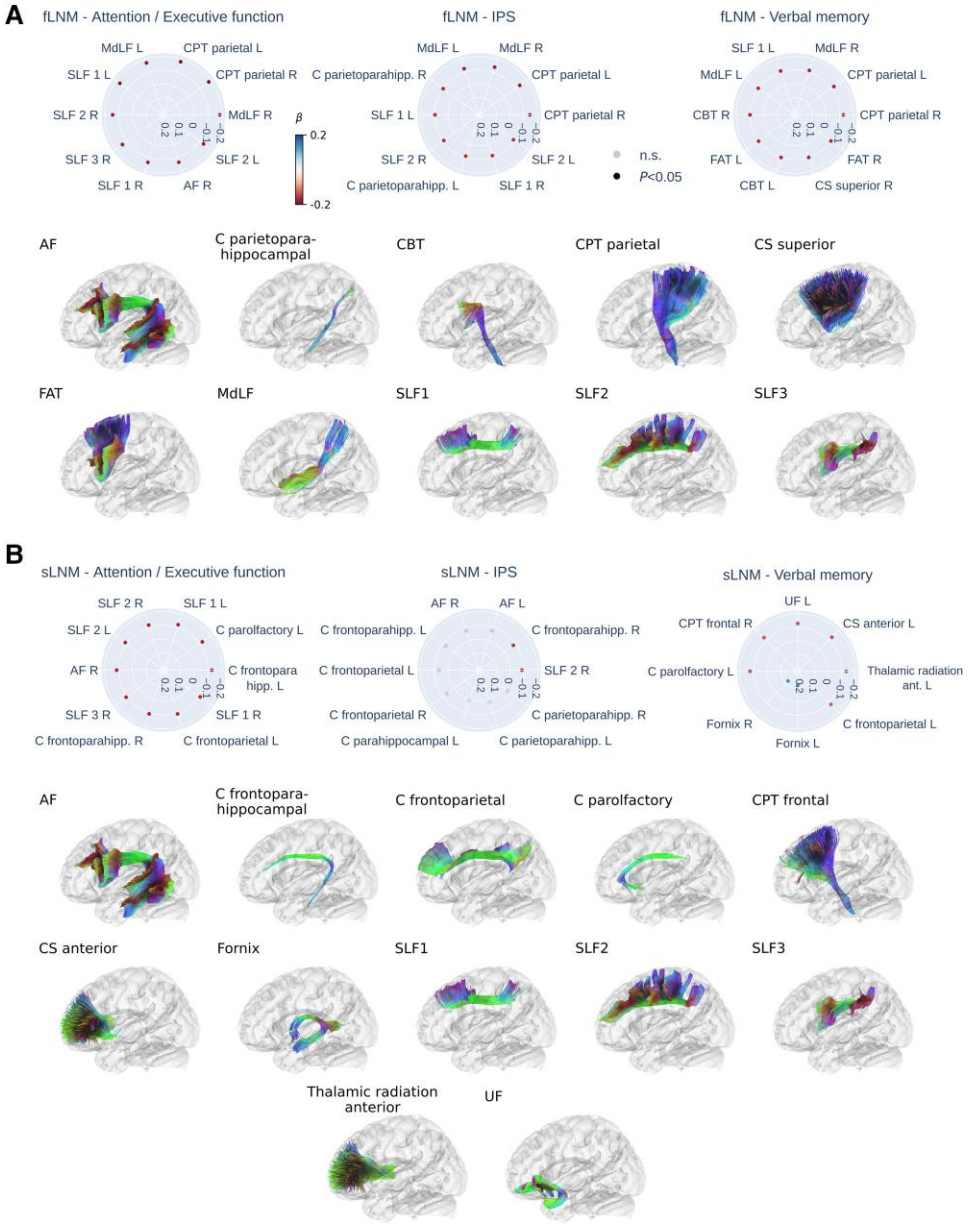

Figure 4 Inferential statistics results of white matter tracts. Radar plots displaying the top 10 strongest linear associations (standardized β) for the functional (**A**) and structural (**B**) lesion network mapping (LNM) scores in each tract in association with cognitive domain scores. Strongest associations are shown at the 3 o'clock position, decreasing in strength counterclockwise. Red dots indicate a negative association (higher LNM score – lower cognitive domain score) and blue dots indicate a positive association (higher LNM score – higher cognitive domain score). Faintly coloured dots indicate non-significant associations. Tracts with a significant association are displayed below the radar plots in alphabetical order. For paired tracts only left side examples are visualized. AF = arcuate fascicle; C = cingulate; CBT = corticobulbar tract; CPT = corticopontine tract; CS = corticostriatal pathway; F = fornix; FAT = frontal aslant tract; MdLF = middle longitudinal fasciculus; SLF = superior longitudinal fasciculus; UF = uncinate fasciculus; fLNM = functional lesion network mapping; IPS = information processing speed; n.s. = non-significant; *P* = *P*-value; sLNM = structural lesion network mapping.

LNM scores surpass WMH volumes in predicting cognitive performance

In current clinical practice, cognitive impairment is often attributed to cerebrovascular disease on the basis of total WMH burden assessed through visual inspection, but interindividual variance in this relationship can lead to diagnostic dilemmas. Previous lesion-symptom mapping studies have demonstrated that strategic WMH locations, specifically in commissural and association tracts, are statistically more likely to be associated with lower cognitive performance.[4,6,7] Our LNM-approach adds to this perspective, not only considering the location of WMH but also integrating them with network connectivity information to capture the WMH network embedding. In our analysis, statistical models capitalizing on LNM scores demonstrated superior performance over those relying on total or tract-level WMH volume in predicting cognitive performance in almost all cognitive domains. Therefore, LNM could be leveraged for improving out-of-sample prediction of cognitive performance over demographics, total WMH volume and strategic WMH location in specific white matter tracts.

Of note, the prediction of cognitive performance improved marginally by adding WMH volumes alone.[38] Comparing the

improvement of imaging-informed models, the usage of fLNM and sLNM scores yielded to a 3- to 7-fold increase in added predictive performance over demographics across the three cognitive domains. Our findings are important, given the longstanding reliance on WMH extent as a primary imaging surrogate marker for cognitive impairment in CSVD. We provide evidence for the role of WMH-related 'covert' network-level effects of chronic vascular injury in cognitive deficits, as indicated previously in studies from smaller clinical or population-based studies.[9,55-57] However, the overall amount of variance explained by WMH, even with the use of network-level metrics, was small (all $R^2 < 0.2$, Supplementary Fig. 4) and unexplained variance in cognitive performance remains, likely due to factors beyond the scope of our study, such as genetic predispositions for neurodegeneration, individual brain network resilience to chronic injury, accumulation of misfolded proteins and changes in brain morphology like cortical atrophy.

Improved prediction of cognitive performance was achieved irrespective of the applied LNM modality. Contrasting prior studies suggesting the inferiority of functional LNM compared to structural approaches for predicting cognitive performance post-stroke,[11,58] our contrary findings might arise from differences in the LNM approach as well as our focus on WMH rather than ischaemic stroke lesions. The ROI-based functional LNM method we used may be more suitable to detect the widespread network disturbances induced by WMH, as opposed to the localized impact of stroke lesions. Notably, fLNM and sLNM scores were positively correlated, suggesting some degree of structure-function coupling that could account for their comparable predictive performance. However, the correlation strength was mostly moderate and prediction performance of fLNM and sLNM differed noticeably across sample sizes. In addition, among LNM-informed models, those incorporating both fLNM and sLNM modalities yielded the strongest results. This suggests that both LNM approaches are equally valuable for achieving a high predictive accuracy in general but might also offer complementary information.

Remarkably, including LNM scores based on both WMH and adjacent normal-appearing white matter—the so-called WMH penumbra—improved predictive performance (Supplementary Fig. 15). This suggests that white matter abnormalities beyond visible lesions contribute to cognitive variance in memory clinic patients, reflecting the notion that cerebrovascular pathology contributing to cognitive impairment is widespread and diffuse.[1] Future analyses leveraging CSVD imaging features beyond WMH should expand on this finding.

Although prediction of almost all cognitive domains was improved by LNM scores, predictive performance for language functions did not exceed that of WMH volumes and demographics. From a network perspective, we argue that this finding might be explained by the relatively confined network of left-lateralized brain regions involved in language functions, which might present lower vulnerability to WMH disconnectivity compared to cognitive functions, such as information processing speed, that rely on a widely distributed network of brain regions.[59] Hence, analyses including patient-level information on structural and functional connectivity that can account for interindividual variability in network configuration should expand on this result. Notably, our sensitivity analyses showed that fLNM scores based on other Schaefer Atlas resolutions (100×7, 200×7) significantly improved language prediction compared to models based on demographics and total WMH volume. This may be because these resolutions better identify language-relevant areas, or more technically, due to lower dimensionality with fewer ROIs, which reduces overfitting. In sum, the slight improvement of WMH-based measures over demographic-based predictions suggests that WMH contribute to a limited extent to variance in language function.

WMH related to cognitive impairment map to attention control networks

WMH are considered to compromise cognitive performance by impacting the function of specific brain networks.[10] To localize these effects, we investigated regional associations between functional and structural LNM scores to cognitive performance. We found that higher LNM scores of cortical areas of the dorsal and ventral attention networks were linked to lower attention and executive function, information processing speed and verbal memory (Fig. 3). Therefore, higher WMH connectivity in these networks is associated with reduced cognitive performance indicating that WMH impair cognitive function by disrupting the respective connecting white matter fibre tracts.

The dorsal attention network—including the frontal eye field, the superior parietal lobule, the intraparietal sulcus and caudal areas of the medial temporal gyrus—governs top-down attention control by enabling voluntary orientation, with increased activity in response to cues indicating the focus location, timing or subject.[60,61] The ventral attention network comprises the ventrolateral frontal cortex, medial areas of the superior frontal cortex and the temporoparietal junction.[49,62] This system exhibits activity increases during bottom-up attention control, i.e. upon detection and orientation to salient targets, especially when they appear in unexpected locations.[60,63] As the effect patterns largely converged on these networks (Supplementary Fig. 9), we argue that WMH affect the cognitive functions emerging from these networks, specifically top-down and bottom-up attention control. This aligns with the observation that deficits in attention and executive function are among the most prominent symptoms in CSVD and VCI in general.[1] Furthermore, prior work demonstrates altered resting state functional connectivity as well as task activation in attention control networks related to CSVD.[10,64,65] Given the covariance of the identified effect patterns, we speculate that WMH contribute to variance in the performance of other cognitive domains, e.g. information processing speed, by affecting the attention demands posited by the corresponding tests.

WMH contribute to cognitive impairment by disrupting frontal and parietal white matter tracts

Regional findings in grey matter areas of the attention control networks are further complemented by white matter tract-level results (Fig. 4). Functional and structural LNM converged on a significant involvement of tracts connecting frontal and parietal areas involved in attention: the dorsal, medial and ventral section of the SLF—which are known to connect the anterior and posterior parts of the dorsal and ventral attention networks, the medial longitudinal fasciculus, the corticopontine tract, frontoparietal sections of the cingulate, the anterior thalamic radiation, the frontal aslant tract and the arcuate fascicle. Although there were some differences in highlighted tracts between functional and structural LNM, this possibly reflects that both approaches capture different aspects of the same anatomy, with sLNM possibly being more sensitive to direct WMH-induced disruption of axonal connections and functional LNM also reflecting effects mediated via polysynaptic brain circuitry.

Strikingly, in the context of verbal memory, structural WMH connectivity pinpointed a distinct set of memory-relevant tracts: the uncinate fascicle, cingulate and fornix. Intriguingly, disruptions in fornix connectivity due to WMH were associated with improved verbal memory in patients, a finding that appears counterintuitive given the fornix's involvement in maintaining memory function. This paradox may be attributable to WMH disrupting inhibitory fibres.

Lesion anticorrelations are associated with cognitive function

The attention control networks are functionally contrasted by the default mode network which shows, instead of being engaged during externally focused tasks, increased activity during internally directed attention and self-referential processes.[66] As a result, the default mode network and the attention control networks are often found to be anticorrelated at rest.[49] This anticorrelation is thought to reflect a fundamental aspect of brain organization and the complex dynamic interplay between the networks is thought to be central for cognitive processing. Resting state fMRI studies in CSVD patients suggest that WMH might affect the DMN and attention network interaction, particularly affecting anterior-posterior communication by disrupting long associative white matter fibre tracts.[10,64] Our findings indicate that stronger anticorrelation between the default mode network and WMH—reflected by more negative fLNM scores—correlates with reduced attention, executive function and processing speed, supporting this hypothesis (Supplementary Figs 11 and 12). Furthermore, by demonstrating that prediction performance is stable if based on negative fLNM scores (Supplementary Fig. 10), our results underscore the notion of anticorrelations yielding biologically and clinically meaningful information.

Clinical implications

Drawing upon a comprehensive LNM analysis in a memory clinic sample of patients with differing extent and aetiology of cognitive impairment, our research converges on a unifying hypothesis: WMH contribute to variance in cognitive functions by disrupting brain circuitry involved in attention control. Our findings not only shed light on the intricate relationships between CSVD, neuroanatomy and cognitive impairment, but they also hint at potential avenues of clinical utilization. The definitive role of CSVD treatments, particularly in precluding cognitive sequelae, is yet to be firmly established. Although there have been promising outcomes related to risk factor modification, particularly blood pressure control,[67,68] pointing towards enhanced cognitive trajectories, clinical trials in VCI require biomarkers to robustly identify vascular contributions to cognitive impairment and vulnerable individuals. Integrating lesion connectivity information into clinical assessments could improve the diagnostic accuracy and help to distinguish between causes of cognitive impairment. Furthermore, leveraging connectivity information could facilitate the identification of subgroups at risk of cognitive disorders through vascular lesions likely to reap the most substantial benefits from medical interventions. As we progress, biomarkers targeting the brain networks affected by WMH could inform preventive and therapeutic interventions.

Strengths and limitations

This study's strength lies in its integration of innovative analytical techniques with a large, multicentric dataset.[69] However, we acknowledge several limitations that warrant consideration when interpreting our findings. The inclusion of selected patient samples in several cohorts may limit generalizability to the broader memory clinic population. Additionally, with most patients being of European ancestry, the generalizability of our findings to other ethnicities remains to be established. Furthermore, despite the harmonization of cognitive and imaging data, biases stemming from variations in data acquisition and processing protocols across sites may have impacted our results. On a technical note, while computing fLNM scores, we sampled resting state BOLD signals in the white matter, typically regarded as noisy and often dismissed as an artefact. However, by integrating it with WMH data, we successfully predicted cognitive performance and demonstrated correlations with structural connectivity information. This challenges the traditional view of the white matter BOLD signal as a mere artefact and supports recent studies—including LNM analyses of white matter lesions in multiple sclerosis—demonstrating that it contains biologically meaningful information.[70-72]

Conclusion

WMH-related brain network connectivity measures significantly improve the prediction of current cognitive performance in memory clinic patients compared to WMH volume or epidemiological factors. Our findings highlight the contribution of WMH disconnectivity, particularly in attention-related brain regions, to vascular cognitive impairment. As this research field progresses, harnessing neuroimaging markers of WMH connectivity in CSVD has the potential to aid individualized diagnostic and therapeutic strategies.

Data availability

Analysis code can be accessed on GitHub (https://github.com/csi-hamburg/2024_petersen_wmh_disconnectivity_memory_clinic). The data that support the findings of this study are available from the project leads on reasonable request (https://metavcimap.org/group/become-a-member/). Restrictions related to privacy and personal data sharing regulations and informed consent may apply.

Acknowledgements

The authors wish to acknowledge all participants of the Meta VCI Map Consortium. We thank Lei Zhao for his contribution to imaging data harmonization of the Meta VCI Map project data. We thank Guido Cammà and Charlotte M. Verhagen for their contribution to the processing of the imaging data. We thank Olivia K.L. Hamilton, Irene M.C. Huenges Wajer, Bonnie Y.K. Lam, Adrian Wong and Xu Xin as members of the Meta VCI Map neuropsychology working group for their advice on neuropsychological data harmonization. ADNI data used in preparation of this article were obtained from the Alzheimer's Disease Neuroimaging Initiative (ADNI) database (adni.loni.usc.edu). As such, the investigators within the ADNI contributed to the design and implementation of ADNI and/or provided data but did not participate in analysis or writing of this report. A complete listing of ADNI investigators can be found at: https://adni.loni.usc.edu/wp-content/uploads/how_to_apply/ADNI_Acknowledgement_List.pdf.

Funding

This work was funded by the Deutsche Forschungsgemeinschaft [DFG, German Research Foundation—Schwerpunktprogramm

2041–454012190 (S.B.E., G.T.), Sonderforschungsbereich 936–178316478–C2 (G.T., B.C.)]; the Meta VCI Map consortium is supported by Vici grant 918.16.616 from ZonMw (G.J.B.) and by Veni grant (project 9150162010055) from ZonMW to J.M.B.; National Institutes of Health (NIH), UCD ADRC NIH awards P30 AG10129 and P30 AG072972 (C.D.); V.V. is supported by JPND-funded E-DADS project (ZonMW project #733051106). ADNI data collection and sharing for this project was funded by the National Institutes of Health (Grant U01 AG024904) and DOD ADNI (Department of Defense award number W81XWH-12-2-0012). ADNI is funded by the National Institute on Aging, the National Institute of Biomedical Imaging and Bioengineering, and through generous contributions from the following: AbbVie, Alzheimer's Association; Alzheimer's Drug Discovery Foundation; Araclon Biotech; BioClinica, Inc.; Biogen; Bristol-Myers Squibb Company; CereSpir, Inc.; Cogstate; Eisai Inc.; Elan Pharmaceuticals, Inc.; Eli Lilly and Company; EuroImmun; F. Hoffmann-La Roche Ltd and its affiliated company Genentech, Inc.; Fujirebio; GE Healthcare; IXICO Ltd.; Janssen Alzheimer Immunotherapy Research & Development, LLC.; Johnson & Johnson Pharmaceutical Research & Development LLC.; Lumosity; Lundbeck; Merck & Co., Inc.; Meso Scale Diagnostics, LLC.; NeuroRx Research; Neurotrack Technologies; Novartis Pharmaceuticals Corporation; Pfizer Inc.; Piramal Imaging; Servier; Takeda Pharmaceutical Company; and Transition Therapeutics. The Canadian Institutes of Health Research is providing funds to support ADNI clinical sites in Canada. Private sector contributions are facilitated by the Foundation for the National Institutes of Health (www.fnih.org). The grantee organization is the Northern California Institute for Research and Education, and the study is coordinated by the Alzheimer's Therapeutic Research Institute at the University of Southern California. ADNI data are disseminated by the Laboratory for Neuro Imaging at the University of Southern California.

Competing interests

F.B. is supported by the NIHR biomedical research center at UCLH. M.D. received honoraria for lectures from Bayer Vital and Sanofi Genzyme, Consultant for Hovid Berhad and Roche Pharma. J.M.P. receives royalties on two neuropsychological tests (Five Digit Test and Visual Association Test; all paid to their organization). G.T. has received fees as consultant or lecturer from Acandis, Alexion, Amarin, Bayer, Boehringer Ingelheim, BristolMyersSquibb/Pfizer, Daichi Sankyo, Portola, and Stryker outside the submitted work.

Supplementary material

Supplementary material is available at *Brain* online.

References

1. Dichgans M, Leys D. Vascular cognitive impairment. *Circ Res*. 2017;120:573-591.
2. Wardlaw JM, Smith EE, Biessels GJ, et al. Neuroimaging standards for research into small vessel disease and its contribution to ageing and neurodegeneration. *Lancet Neurol*. 2013;12:822-838.
3. Duering M, Biessels GJ, Brodtmann A, et al. Neuroimaging standards for research into small vessel disease—Advances since 2013. *Lancet Neurol*. 2023;22:602-618.
4. Biesbroek JM, Weaver NA, Hilal S, et al. Impact of strategically located white matter hyperintensities on cognition in memory clinic patients with small vessel disease. *PLoS One*. 2016;11:e0166261.
5. Kloppenborg RP, Nederkoorn PJ, Geerlings MI, van den Berg E. Presence and progression of white matter hyperintensities and cognition: A meta-analysis. *Neurology*. 2014;82:2127-2138.
6. Coenen M, Kuijf HJ, Huenges Wajer IMC, et al. Strategic white matter hyperintensity locations for cognitive impairment: A multicenter lesion-symptom mapping study in 3525 memory clinic patients. *Alzheimers Dement*. 2023;19:2420-2432.
7. Duering M, Gesierich B, Seiler S, et al. Strategic white matter tracts for processing speed deficits in age-related small vessel disease. *Neurology*. 2014;82:1946-1950.
8. Seiler S, Fletcher E, Hassan-Ali K, et al. Cerebral tract integrity relates to white matter hyperintensities, cortex volume, and cognition. *Neurobiol Aging*. 2018;72:14-22.
9. ter Telgte A, van Leijsen EMC, Wiegertjes K, Klijn CJM, Tuladhar AM, de Leeuw FE. Cerebral small vessel disease: From a focal to a global perspective. *Nat Rev Neurol*. 2018;14:387-398.
10. Dey AK, Stamenova V, Turner G, Black SE, Levine B. Pathoconnectomics of cognitive impairment in small vessel disease: A systematic review. *Alzheimers Dement*. 2016;12:831-845.
11. Salvalaggio A, De Filippo De Grazia M, Zorzi M, Thiebaut de Schotten M, Corbetta M. Post-stroke deficit prediction from lesion and indirect structural and functional disconnection. *Brain*. 2020;143:2173-2188.
12. Foulon C, Cerliani L, Kinkingnéhun S, et al. Advanced lesion symptom mapping analyses and implementation as BCBtoolkit. *Gigascience*. 2018;7:1-17.
13. Jiang J, Bruss J, Lee WT, Tranel D, Boes AD. White matter disconnection of left multiple demand network is associated with post-lesion deficits in cognitive control. *Nat Commun*. 2023;14:1740.
14. Talozzi L, Forkel SJ, Pacella V, et al. Latent disconnectome prediction of long-term cognitive-behavioural symptoms in stroke. *Brain*. 2023;146:1963-1978.
15. Siddiqi SH, Kletenik I, MC A, et al. Lesion network localization of depression in multiple sclerosis. *Nat Mental Health*. 2023;1:36-44.
16. Weaver NA, Zhao L, Biesbroek JM, et al. The meta VCI map consortium for meta-analyses on strategic lesion locations for vascular cognitive impairment using lesion-symptom mapping: Design and multicenter pilot study. *Alzheimers Dement (Amst)*. 2019;11:310-326.
17. Jack CR, Barnes J, Bernstein MA, et al. Magnetic resonance imaging in Alzheimer's disease neuroimaging initiative 2. *Alzheimers Dement*. 2015;11:740-756.
18. Hinton L, Carter K, Reed BR, et al. Recruitment of a community-based cohort for research on diversity and risk of dementia. *Alzheimer Dis Assoc Disord*. 2010;24:234-241.
19. Case NF, Charlton A, Zwiers A, et al. Cerebral amyloid angiopathy is associated with executive dysfunction and mild cognitive impairment. *Stroke*. 2016;47:2010-2016.
20. Pusswald G, Lehrner J, Hagmann M, et al. Gender-specific differences in cognitive profiles of patients with Alzheimer's disease: Results of the prospective dementia registry Austria (PRODEM-Austria). *J Alzheimers Dis*. 2015;46:631-637.
21. Boomsma JMF, Exalto LG, Barkhof F, et al. Vascular cognitive impairment in a memory clinic population: Rationale and design of the "Utrecht-Amsterdam clinical features and prognosis in vascular cognitive impairment" (TRACE-VCI) study. *JMIR Res Protoc*. 2017;6:e60.
22. Weaver NA, Kuijf HJ, Aben HP, et al. Strategic infarct locations for post-stroke cognitive impairment: A pooled analysis of individual patient data from 12 acute ischaemic stroke cohorts. *Lancet Neurol*. 2021;20:448-459.

23. Kuijf HJ, Biesbroek JM, De Bresser J, et al. Standardized assessment of automatic segmentation of white matter hyperintensities and results of the WMH segmentation challenge. *IEEE Trans Med Imaging*. 2019;38:2556-2568.
24. Biesbroek JM, Kuijf HJ, Weaver NA, et al. Brain infarct segmentation and registration on MRI or CT for lesion-symptom mapping. *J Vis Exp*. 2019;151:e59653.
25. Yeh FC. Population-based tract-to-region connectome of the human brain and its hierarchical topology. *Nat Commun*. 2022; 13:4933.
26. Coenen M, Biessels GJ, DeCarli C, et al. Spatial distributions of white matter hyperintensities on brain MRI: A pooled analysis of individual participant data from 11 memory clinic cohorts. *Neuroimage Clin*. 2023;40:103547.
27. Horn A, Reich M, Vorwerk J, et al. Connectivity predicts deep brain stimulation outcome in Parkinson disease. *Ann Neurol*. 2017;82:67-78.
28. Joutsa J, Moussawi K, Siddiqi SH, et al. Brain lesions disrupting addiction map to a common human brain circuit. *Nat Med*. 2022;28:1249-1255.
29. Schaefer A, Kong R, Gordon EM, et al. Local-global parcellation of the human cerebral cortex from intrinsic functional connectivity MRI. *Cerebral Cortex*. 2018;28:3095-3114.
30. Tian Y, Margulies DS, Breakspear M, Zalesky A. Topographic organization of the human subcortex unveiled with functional connectivity gradients. *Nat Neurosci*. 2020;23: 1421-1432.
31. Cohen A, Soussand L, McManus P, Fox M. GSP1000 preprocessed connectome. Harvard Dataverse. Published online 17 April 2021. doi:10.7910/DVN/ILXIKS
32. Cohen A, Al-Fatly B, Horn A. GSP1000 preprocessed connectome for lead DBS. Harvard Dataverse. Published online 2 February 2024. doi:10.7910/DVN/KKTJQC
33. Yeo BTT, Krienen FM, Sepulcre J, et al. The organization of the human cerebral cortex estimated by intrinsic functional connectivity. *J Neurophysiol*. 2011;106:1125-1165.
34. Neudorfer C, Butenko K, Oxenford S, et al. Lead-DBS v3.0: Mapping deep brain stimulation effects to local anatomy and global networks. *NeuroImage*. 2023;268:119862.
35. Yeh F-C, Wedeen VJ, Tseng WYI. Generalized q-sampling imaging. *IEEE Trans Med Imaging*. 2010;29:1626-1635.
36. Hamdan S, More S, Sasse L, et al. Julearn: An easy-to-use library for leakage-free evaluation and inspection of ML models. *Gigabyte*. 2024;2024:1-16.
37. Abraham A, Pedregosa F, Eickenberg M, et al. Machine learning for neuroimaging with scikit-learn. *Front Neuroinform*. 2014;8:14.
38. Poldrack RA, Huckins G, Varoquaux G. Establishment of best practices for evidence for prediction: A review. *JAMA Psychiatry*. 2020;77:534-540.
39. Padmanabhan JL, Cooke D, Joutsa J, et al. A human depression circuit derived from focal brain lesions. *Biol Psychiatry*. 2019;86: 749-758.
40. Bos D, Ikram MA. Research aims in clinical medicine: Description, identification, or explanation. *World Neurosurg*. 2022;161:240-244.
41. Omidvarnia A, Sasse L, Larabi DI, et al. Individual characteristics outperform resting-state fMRI for the prediction of behavioral phenotypes. *Commun Biol*. 2024;7:771.
42. Varoquaux G, Raamana PR, Engemann DA, Hoyos-Idrobo A, Schwartz Y, Thirion B. Assessing and tuning brain decoders: Cross-validation, caveats, and guidelines. *NeuroImage*. 2017; 145:166-179.
43. Nadeau C, Bengio Y. Inference for the generalization error. *Mach Learn*. 2003;52:239-281.
44. Vallat R. Pingouin: Statistics in python. *J Open Source Softw*. 2018; 3:1026.
45. Winkler AM, Ridgway GR, Webster MA, Smith SM, Nichols TE. Permutation inference for the general linear model. *Neuroimage*. 2014;92:381-397.
46. Markello RD, Hansen JY, Liu ZQ, et al. Neuromaps: Structural and functional interpretation of brain maps. *Nat Methods*. 2022;19:1472-1479.
47. Alexander-Bloch AF, Shou H, Liu S, et al. On testing for spatial correspondence between maps of human brain structure and function. *NeuroImage*. 2018;178:540-551.
48. Margulies DS, Ghosh SS, Goulas A, et al. Situating the default-mode network along a principal gradient of macroscale cortical organization. *Proc Natl Acad Sci U S A*. 2016;113:12574-12579.
49. Fox MD, Snyder AZ, Vincent JL, Corbetta M, Van Essen DC, Raichle ME. The human brain is intrinsically organized into dynamic, anticorrelated functional networks. *Proc Natl Acad Sci U S A*. 2005;102:9673-9678.
50. Fox MD, Zhang D, Snyder AZ, Raichle ME. The global signal and observed anticorrelated resting state brain networks. *J Neurophysiol*. 2009;101:3270-3283.
51. Maillard P, Fletcher E, Harvey D, et al. White matter hyperintensity penumbra. *Stroke*. 2011;42:1917-1922.
52. Mayer C, Nägele FL, Petersen M, et al. Free-water diffusion MRI detects structural alterations surrounding white matter hyperintensities in the early stage of cerebral small vessel disease. *J Cereb Blood Flow Metab*. 2022;42:1707-1718.
53. Pustina D, Avants B, Faseyitan OK, Medaglia JD, Coslett HB. Improved accuracy of lesion to symptom mapping with multivariate sparse canonical correlations. *Neuropsychologia*. 2018; 115:154-166.
54. Bowren M, Adolphs R, Bruss J, et al. Multivariate lesion-behavior mapping of general cognitive ability and its psychometric constituents. *J Neurosci*. 2020;40:8924-8937.
55. De Luca A, Kuijf H, Exalto L, Thiebaut de Schotten M, Biessels GJ. Multimodal tract-based MRI metrics outperform whole brain markers in determining cognitive impact of small vessel disease-related brain injury. *Brain Struct Funct*. 2022;227: 2553-2567.
56. Frey BM, Petersen M, Schlemm E, et al. White matter integrity and structural brain network topology in cerebral small vessel disease: The Hamburg city health study. *Hum Brain Mapp*. 2021;42:1406-1415.
57. Schlemm E, Frey BM, Mayer C, et al. Equalization of brain state occupancy accompanies cognitive impairment in cerebral small vessel disease. *Biol Psychiatry*. 2022;92:592-602.
58. Pini L, Salvalaggio A, De Filippo De Grazia M, Zorzi M, Thiebaut de Schotten M, Corbetta M. A novel stroke lesion network mapping approach: Improved accuracy yet still low deficit prediction. *Brain Commun*. 2021;3:fcab259.
59. Friederici AD. The brain basis of language processing: From structure to function. *Physiol Rev*. 2011;91:1357-1392.
60. Corbetta M, Kincade JM, Ollinger JM, McAvoy MP, Shulman GL. Voluntary orienting is dissociated from target detection in human posterior parietal cortex. *Nat Neurosci*. 2000;3: 292-297.
61. Shulman GL, McAvoy MP, Cowan MC, et al. Quantitative analysis of attention and detection signals during visual search. *J Neurophysiol*. 2003;90:3384-3397.
62. Alves PN, Forkel SJ, Corbetta M, Thiebaut de Schotten M. The subcortical and neurochemical organization of the ventral and dorsal attention networks. *Commun Biol*. 2022;5:1343.
63. Astafiev SV, Shulman GL, Stanley CM, Snyder AZ, Van Essen DC, Corbetta M. Functional organization of human intraparietal and

frontal cortex for attending, looking, and pointing. *J Neurosci*. 2003;23:4689-4699.
64. Schulz M, Malherbe C, Cheng B, Thomalla G, Schlemm E. Functional connectivity changes in cerebral small vessel disease—A systematic review of the resting-state MRI literature. *BMC Med*. 2021;19:103.
65. Ding JR, Ding X, Hua B, et al. Altered connectivity patterns among resting state networks in patients with ischemic white matter lesions. *Brain Imaging Behav*. 2018;12:1239-1250.
66. Greicius MD, Krasnow B, Reiss AL, Menon V. Functional connectivity in the resting brain: A network analysis of the default mode hypothesis. *Proc Natl Acad Sci U S A*. 2003;100:253-258.
67. SPRINT MIND Investigators for the SPRINT Research Group; Williamson JD, Pajewski NM, et al. Effect of intensive vs standard blood pressure control on probable dementia: A randomized clinical trial. *JAMA*. 2019;321:553-561.
68. Veronese N, Facchini S, Stubbs B, et al. Weight loss is associated with improvements in cognitive function among overweight and obese people: A systematic review and meta-analysis. *Neurosci Biobehav Rev*. 2017;72:87-94.
69. Marek S, Tervo-Clemmens B, Calabro FJ, et al. Reproducible brain-wide association studies require thousands of individuals. *Nature*. 2022;603:654-660.
70. Schilling KG, Li M, Rheault F, et al. Whole-brain, gray, and white matter time-locked functional signal changes with simple tasks and model-free analysis. *Proc Natl Acad Sci U S A*. 2023;120:e2219666120.
71. Baller EB, Sweeney EM, Cieslak M, et al. Mapping the relationship of white matter lesions to depression in multiple sclerosis. *Biol Psychiatry*. 2024;95:1072-1080.
72. Kletenik I, Cohen AL, Glanz BI, et al. Multiple sclerosis lesions that impair memory map to a connected memory circuit. *J Neurol*. 2023;270:5211-5222.